Materials Today Chemistry 35 (2024) 101855

Contents lists available at ScienceDirect

Materials Today Chemistry

journal homepage: www.journals.elsevier.com/materials-today-chemistry/

Melanin-inspired conductive thin films for multimodal-sensing wearable on-skin electronics

Noemí Contreras-Pereda [a], Salvio Suárez-García [a], Raphael Pfattner [b], Daniel Ruiz-Molina [a,*]

[a] Catalan Institute of Nanoscience and Nanotechnology (ICN2), CSIC and BIST, Campus UAB, Bellaterra, Barcelona, 08193, Spain
[b] Institut de Ciència de Materials de Barcelona, ICMAB-CSIC, Campus UAB, Bellaterra, 08193, Spain

ARTICLE INFO

Keywords:
Melanin-inspired
Wearable devices
e-skin
Thin films

ABSTRACT

Electronic skins (e-skins), composed of various flexible sensors, mimic the sensing functions of human skin aiming for both healthcare monitoring and prosthetics development applications. So far different multi-component e-skin devices aimed to fulfill different requirements (biocompatibility, skin adhesion, flexibility, conductivity, sensitivity towards biological stimuli and stretchability) have been reported. However, the obtaining of such devices combining all the above requirements within a single material that simplifies not only cost but specially functioning still remains a challenge. For this, catechol-based materials have attracted special attention due to their adhesive properties, compatibility and melanin-like electrical conduction. In this work, 2,3,6,7,10,11 – hexahydroxy triphenylene (HHTP) was used as catechol moiety in a typical melanin-like polymerization, resulting in a free-standing melanin-inspired film (MN-film). The obtained MN-film showcased good conductivities with dual charge carriers (electrons and ions) under different environments, *i.e.* pure water and buffers simulating sweat. Large biocompatibility, adhesion and conformability to skin were obtained as well, allowing to implement the film in wearable electronic on-skin devices on porcine skin. Measurements in wearable devices indicated large sensitivity towards different stimuli (strain, motion and temperature) under sweat-like conditions.

1. Introduction

In the recent years, bioelectronics has emerged as ground-breaking field with several point-of-care applications more notably on skin, henceforth referred as e-skin devices [1,2]. Conformability and strain-dependent electrical conductance of e-skin and wearable devices have opened the way to remarkable applications as body motion [3], tactile sensors or monitoring of bodily electrical signals as electromyography or electrocardiography (ECG) [4] or cardiac ultrasound [5]. On top of that, physiological recording of parameters such as temperature, light, respiratory and humidity is giving rise to human-machine interfaces for artificial intelligence and precise movement control of prosthetics [6–8]. Commercial skin electrodes commonly used nowadays in medical monitoring are typically rigid and made with conventional conductors, though their characteristics are still far from the needs of ideal e-skin devices. First, these electrodes are conformed of rigid metal pads implemented on the skin with aggressive gels and adhesives [9]. Further than the possibility of causing skin or allergic irritation, these planar electrodes do not properly adapt to the skin roughness and wrinkled surface lacking in conformability [6,10]. The subsequent voids between the skin and the electrode not only lead to a large electrical impedance, hindering thus the electronic monitoring, but also implies a very low electrode adhesion and consequently short-term stable recording [11]. Moreover, current commercial electrodes are not suitable during intensive body performance as they have proven to not be water or sweat resistant [12]. Thus, novel materials for e-skin devices have been sought.

Said materials should meet several characteristics, mainly though not exclusively: I) robust skin adhesion [13,14], preferably with a large conformability to the skin surface and/or large elasticity and stretchability to adapt to body shapes and follow movements [1,9], II) should have low electrical contact impedance with skin (typically below 20 kΩ) to ensure good electrical contact during the bodily signal measurement [6,9] and last but not least, III) be water-proof with resistant adhesion to skin under wet or sweat like conditions.

Natural hydrogels with bioadhesive and self-healing properties have been reported in numerous and interesting health care applications [15]. Their remarkable stiffness modulus and high hydrophilicity made

* Corresponding author.
E-mail address: dani.ruiz@icn2.cat (D. Ruiz-Molina).

https://doi.org/10.1016/j.mtchem.2023.101855
Received 28 August 2023; Received in revised form 2 November 2023; Accepted 9 December 2023
Available online 12 December 2023
2468-5194/© 2023 The Authors. Published by Elsevier Ltd. This is an open access article under the CC BY-NC-ND license (http://creativecommons.org/licenses/by-nc-nd/4.0/).

them also very attractive for e-skin devices [10], though due to their lack of inherent carrier conduction they often require doping to enhance electrical conductivity [4]. Free-standing conductive thin films compatible with current device fabrication techniques represents a noteworthy alternative [12,16]. The reported devices are principally based on multilayered stacked thin films, performing each layer a different and distinct functionality, from adhesion to conduction. For instance, Ding and co-workers developed a highly elastic and breathable e-skin device, exhibiting a large pressure sensibility within the 0–175 kPa range, upon superposition of a highly elastic fibrous polyurethane, a conductive carbon fiber layer and a polyvinylidene fluoride triboelectric sensing coating [17]. In another example, Chen and co-workers introduced a bubble-like stretchable *Janus* thin film with high adhesion to the skin surface that enabled body motion, breathing and pneumatic monitoring [18]. The film comprised a hydrophilic/hydrophobic interphase as it consisted of a polydimethylsiloxane (PDMS) layer introduced over a carbon nanotube thin film. Similar devices were reported by Xue and co-workers [19]. The material synthetized at liquid-air interface consisted of a carbon nanotube thin film coated by a thermoelastic polymer on its upside layer and by PDMS on the water-side layer. The PDMS coating enhanced the hydrophobicity of the film whereas the thermoelastic polymer conferred it a large strain resistance. The device was used as pulse and movement sensor with large and stable performance under different wetting conditions, pHs and presence of salts or alkali, suggesting compatibility with sweat during body motion.

Beyond multilayered devices, wearable electronics conformed by a unique single material will represent an ideal scenario if we really want to simplify the operation and manufacturing costs. However, it is not easy to design a solid material that meets all the previously mentioned conditions of conductivity, flexibility, adhesion, and strength.

To achieve this objective, we hypothesize that melanin-inspired thin films can arise as competitive candidates. Eumelanin are natural pigments with a contrasted biocompatibility and inherent ionic conduction in the wet state and electronic conduction in the dry state [20–22]. On top of that, main building blocks of eumelanin composition are catechol groups, which confer good adhesive properties over a wide variety of surfaces even in aqueous environments [21] to tissues [23] and skin for wound healing [24]. Notoriously, inclusion of catechol moieties and polydopamine in wearable electronics has already been explored both in hydrogels [25–27] and multifunctional thin films [28,29]. Exemplarily, tannic acid was included in an acrylamide and cellulose based hydrogel (doped with silver ions to enhance electrical conduction for body motion detection) proving to be a good adhesive [25]. On the other hand, polydopamine derived polymers were used as adhesive layer of on-skin electrodes for ECG monitoring with a high skin conformability but also long-term stable heartbeat recording, including monitoring during intense exercise [29] and under-water activity [28]. Nonetheless, good electrical conduction of these electrodes was achieved by depositing a conductive gold layer on top of the polydopamine-based polymer, coated by a hydrophobic polymer due to the low conductivity of the adhesive layer alone. Though, as far as we know, no single sticky catechol-based thin-film with good electrical conductivity for developing e-skin devices has been described.

Herein we have achieved this objective upon the melanin-like polymerization of the tris-catechol 2,3,6,7,10,11-hexahydroxytriphenylene (HHTP). The electronic delocalization of the aromatic core, already used to prepare conductive Metal-Organic Frameworks (MOFs) and Covalent Organic Frameworks (COFs), is intended to confer additional conductive properties to melanin-like polymers [30]. The resulting free-standing melanin-inspired film (MN-film) exhibits dual charge carrier conduction mechanisms, great biocompatibility and adhesion to skin of the MN-films, which prompted their use as e-skin devices that monitor multiple bodily signals.

2. Results and discussion

Melanin-like polymerization is achieved from the crosslinking between catechol groups and bis-amine molecules as nitrogen base species [31]. First experiments were done by directly mixing carbonate aqueous buffer solutions of HHTP and PPD (for more info in the reference protocol see Supporting Information Fig. S1). The overall solution turned immediately brown as an indicator of melanin-like polymerization. Within minutes, sub-millimeter sized thin films were already observed in the water-air interface and remained of similar sizes after 24 h indicating a fast nucleation and polymerization. Likely, analogous reactions performed with methanolic solutions did not lead to observable films nor precipitation at naked eye not even after 24 h (see Supporting Information Fig. S2a). However, upon drop casting of the suspension, thin plate-like particles with micrometer range lateral could be observed with scanning electron microscopy (SEM) after solvent evaporation (see Supporting Information Fig. S2b).

Due to the partial failure of these approaches, liquid-liquid interfacial approach was pursued afterwards to ensure a controlled slow polymerization. For this, HHTP was reacted with *p*-phenylenediamine (PPD) using an interfacial polymerization, a well-known methodology for the fabrication of functional COF films (see Fig. 1) [30]. The synthetic protocol consists in pouring a saturated ethyl acetate solution of HHTP over an aqueous solution of PPD, ensuing a centimeter long brown film on top of the aqueous phase (see Supporting Information Fig. S3). The obtained films presented a Janus character (with a more rough but adhesive surface on the water side and a smooth surface on the ethyl acetate face). Additionally, the film showed a not negligible conductance though it was critically affected by several grain boundaries and defects created upon film manipulation while the films were too brittle to be free-standing as already observed in previously described melanin-inspired films [32].

So, the reaction was repeated including now Xanthan Gum as biocompatible additive, creating a liquid-liquid interface for slow diffusion of HHTP into the aqueous phase. After three days of reaction, the remaining ethyl acetate solution was removed finding the free-standing melanin-like film (MN-film) on top of the aqueous phase (see Supporting Information Fig. S4). Remarkably, the MN-films proved to be considerably thin, very flexible, and highly stable under wetting conditions. In fact, a film expanded over the water-air interface upon contact with water remains stable without suffering structural damages for weeks. Scanning electron microscopy (SEM) images (Fig. 1b) showed a smooth and crack-free surface with lateral sizes in the centimeter range. The FT-IR spectrum of MN-films (Fig. 1c) showed a wide absorption peak at ~3300 cm^{-1} corresponding to the largely energetic ν(O–H) from HHTP and a peak at ~1500 cm^{-1} associated the ν(C–N) band of the PPD. Additional peaks from the δ(O–H) and δ(N–H) groups are seen at ~1620 cm^{-1} though shifted to lower wavenumbers (~20 cm^{-1} shift) with respect to the free HHTP and PPD, fact attributed to its participation in the polymerization process [31]. Additional ν(C–H) vibrations at ~2920 cm^{-1} and suppression of the peaks at 1720 and 1600 cm^{-1} corresponding to the δ(O–H) modes may indicate the incorporation of the Xanthan Gum.

Finally, and worth to mention, the side of the MN-film facing the water phase along the synthesis is high hydrophilicity; in contact with water expands while upon exposition to air after pulling the MN-film out of the interface induces its folding (see Video S1 in the Supplementary Information and Fig. 1d). This process can be reversibly repeated several times without damaging, indicating a large robustness but when trying to recover the film by fishing on top of a silicon substrate, the film avoids contact with the surface remaining at the water-air interface (see Video S2 in the Supplementary Information). On the contrary, the film side facing the ethyl acetate phase along the synthesis resulted more hydrophobic so it remains folded in contact with water.

To assess the skin adhesion properties, our film was deposited on top of wetted untreated porcine skin and the excess of water was gently

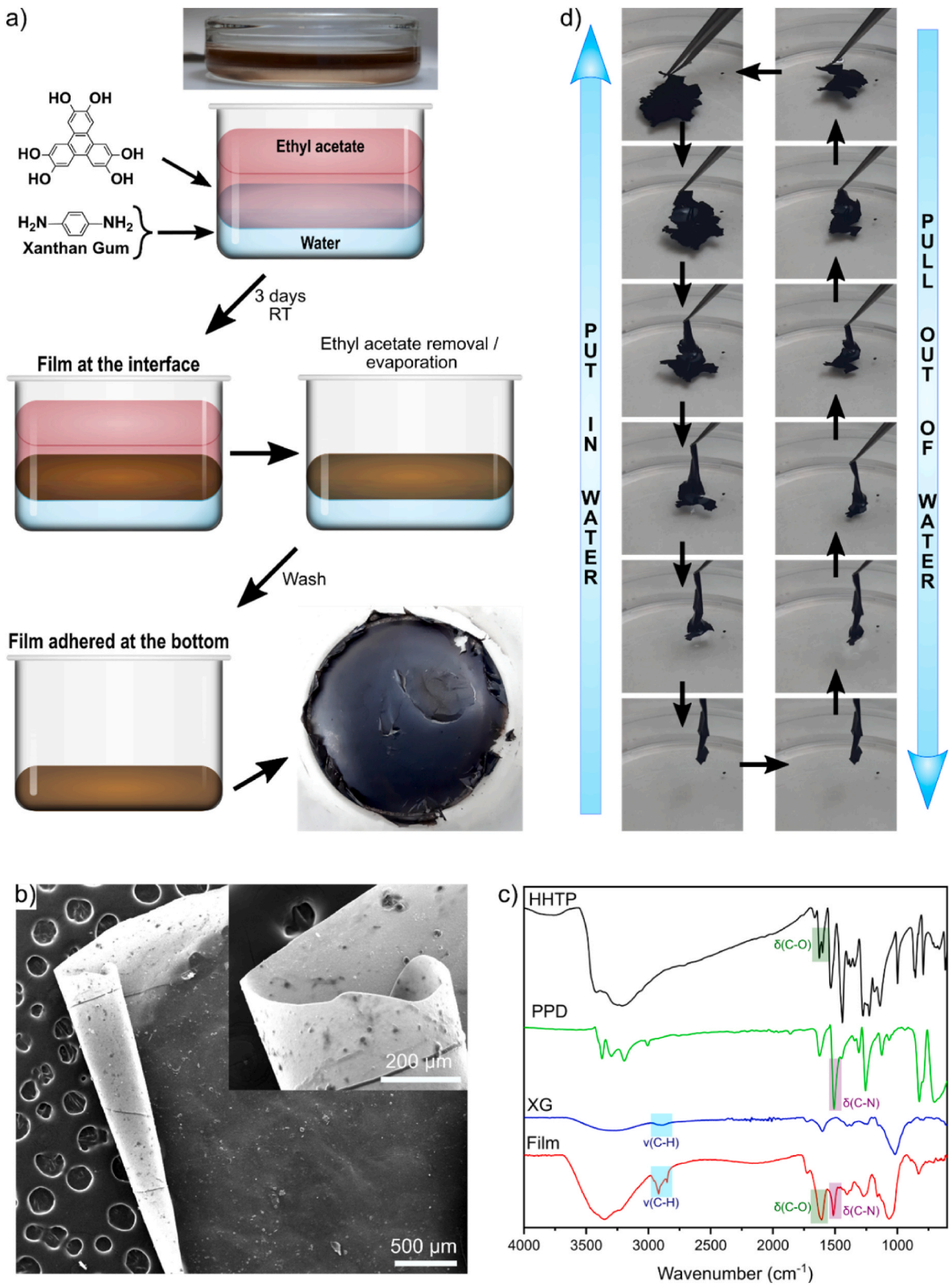

Fig. 1. (a) Synthetic protocol for the obtaining of the free-standing MN-film. (b) SEM images of the free-standing MN-film. (c) Comparative IRs of the free-standing MN-film and the starting reagents. (d) The MN-film deposited at the water-air interface in a water-filled Petri dish was pulled in and out repeatedly, observing its folding into a fibre upon pulling out of the water, avoiding exposing its hydrophilic surface.

removed with a tissue. The film remained on the skin with high adhesion imitating the natural melanin pigmentation (Fig. 2a) both under wet and dry conditions, reproducing the complex skin surface and adapting to its wrinkles and porosities (Fig. 2b).

Moreover, the film can be shaped with different designs aiming for personalized tattoo-like e-skin electrodes (Fig. 2h and i). For instance, circular shapes could be obtained upon using a circular puncher cutter (Fig. 2h) or even more complex butterfly-like forms upon manual cutting (Fig. 2i). Interestingly, when the porcine skin was stretched and deformed reproducing typical skin stresses (see Video S3 in Supporting Information and Fig. 2c–f) the adhesive capabilities nor the conformability of the film to the skin was modified, as shown by the inset of Fig. 2h. Finally, waterproofing of the on-skin adhered films was tested on the hand of a volunteer, moving it underneath water. Worth-to-mention, the film remained adhered to the skin when immersing and withdrawing the hand in water and when moving the hand side-to-side underneath steady water flow (see Video S4 in Supporting Information and Fig. 2g). Nevertheless, the film can be reversibly removed under high flows of warm water for a prolonged period of time (see Video S5 in Supporting Information and Fig. S5). In any case, the biocompatibility and low toxicity was confirmed by culturing 3 mm in diameter disks of MN-films with epithelial fibroblast cells for 24 h. Cell viability was measured to be 90.14 ± 2.35 % suggesting high biocompatibility and lack of possible skin irritation (Fig. 3d). Besides, considering the topical

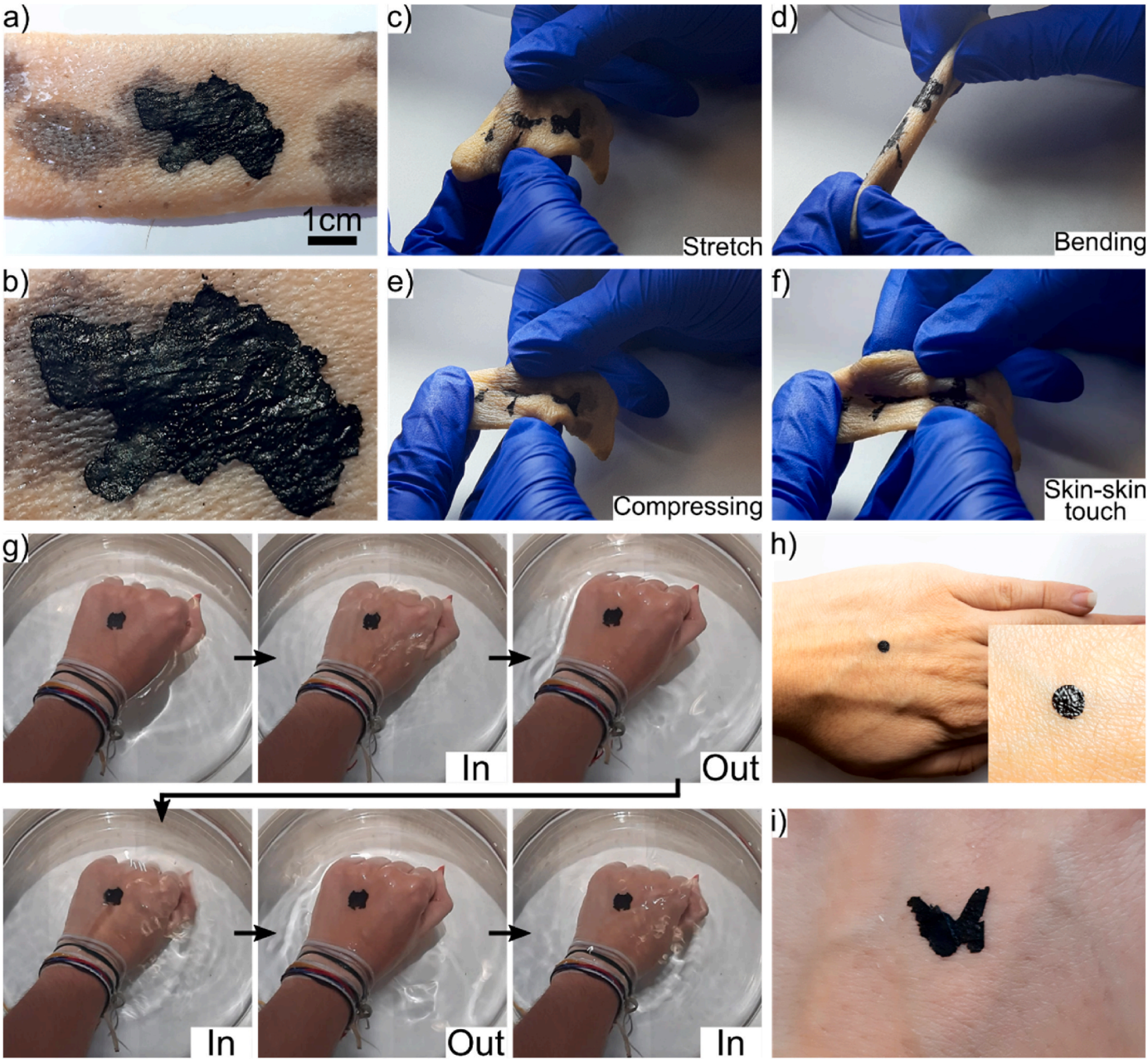

Fig. 2. (a) Photograph of MN-films adhered on pork skin. The light brown stains correspond to natural melanin pigmentation of the skin. (b) Magnified picture of the MN-films adhered on pork skin showing the large conformability imitating the skin pigmentation to the skin. Natural wrinkles of the skin are well reproduced. (c–f) Photographs of pork skin deformations with e-skin devices of different sizes on top. Skin deformations are indicated on the picture: Stretching, bending and compressing of the skin and skin-skin touch with the film in the middle. (g) Photographs extracted from a video. MN-film was previously deposited on the volunteer's hand. The hand was pulled in and out of a water bath repeatedly. MN-film remained adhered to the skin. (h) and (i) Photographs of circular and butterfly-shaped MN-films deposited on a volunteer's hand. (For interpretation of the references to color in this figure legend, the reader is referred to the Web version of this article.)

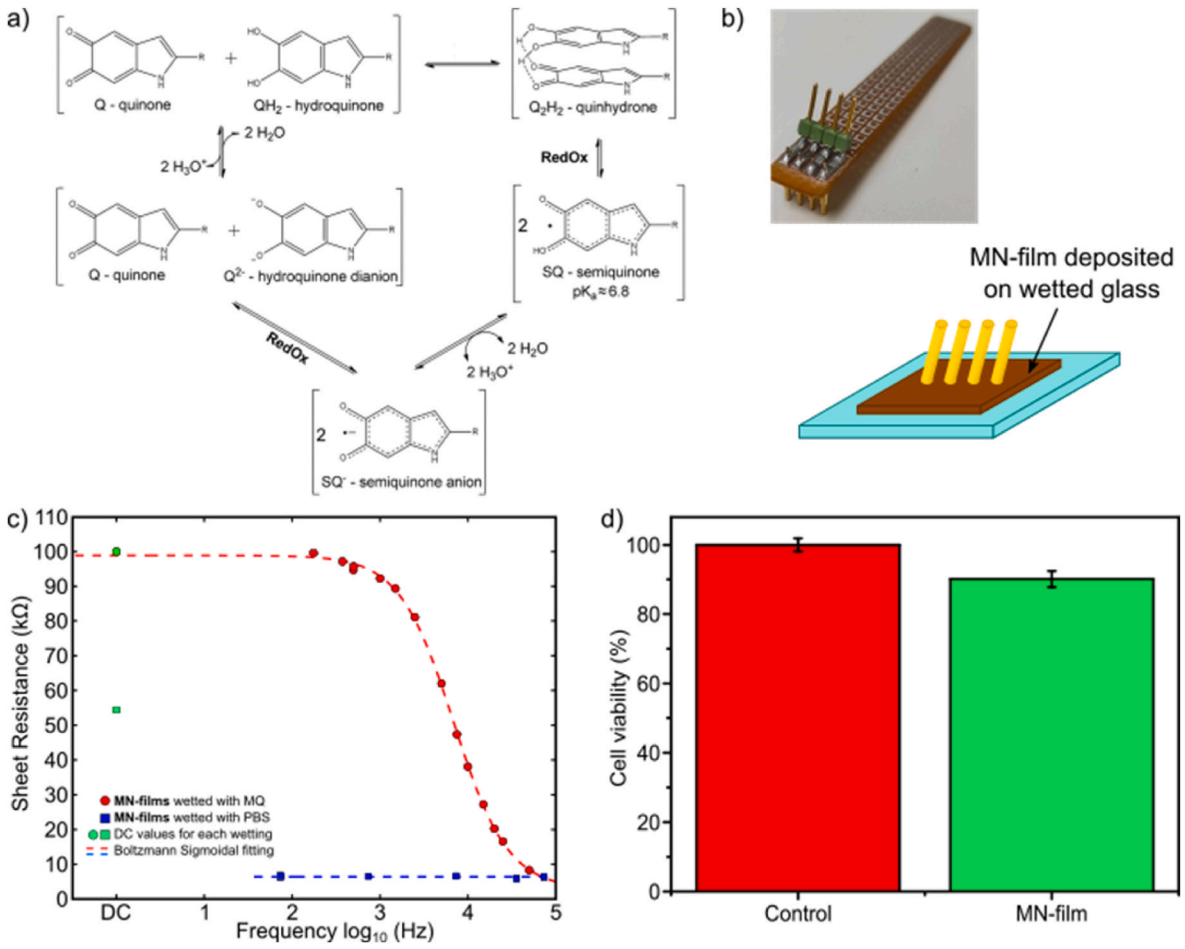

Fig. 3. (a) Scheme on redox reactions occurring within eumelanin in the presence of water. Adapted with permission [33]. Copyright 2019, RSC Advances. Several states are either ionic or radical species which justify the enhanced conductivity in the wetted state and the ionic conduction. (b) Insets: Photograph of four-wire spring loaded indentation electrodes and scheme of the measurement. (c) AC frequency dependence and DC sheet resistances of MN- films wetted with pure MQ water (red curve) and physiological sweat-like PBS buffer (blue curve). (d) Fibroblast cell viability in presence of the MN-films. (For interpretation of the references to color in this figure legend, the reader is referred to the Web version of this article.)

application, the MN-film was put in contact with the skin of volunteers for 24 h. As a result, no signs of inflammation, irritation or erythema were observed on the skin.

As both electron and ion conduction are expected, frequency dependent electrical AC measurements were also tested using a Lock-in amplifier system [34] and four-wire spring loaded indentation contacts on flat films deposited on insulating glass substrates that minimize mechanical stress under wetting conditions (Fig. 3b). As seen in the sheet resistance variation with the frequency (Fig. 3c red curve), films at 100 % RH (*i.e.* fully wetted in water) exhibited two conduction regimes depending on the applied frequency corresponding to the two plateau of the Boltzmann sigmoidal. At low frequencies, high sheet resistances are obtained stabilizing at $R_{sheet} = 98 \pm 2$ kΩ. Worth-to-mention, the sheet resistance at low frequencies converges to the value obtained when measuring the wet thin film in conventional four-wire DC measurements with the same contacts. This region corresponds to mostly electronic conduction as constant currents in the DC regime disable proton and ion conduction through full polarization of water molecules and ionic species (*i.e.* electrode polarization). On the other hand, at high frequencies, the sheet resistance critically decreases, reaching values of $R_{sheet} = 3 \pm 2$ kΩ, confirming the contribution of both electron and proton charge carrier conduction. Observation of a steady plateau at higher frequencies could not be obtained due to the limitations of the setup: as observed during calibration of the equipment with high precision commercial resistors, interferences in the signal coming from copper cabling arise at frequencies higher than 73.5 kHz. Considering the thickness of the film (7 ± 2 μm as observed in SEM images), conductivity values of $\sigma = 15 \pm 4$ mS cm^{-1} and $\sigma = 0.5 \pm 0.2$ S cm^{-1} are obtained respectively for low and high frequency ranges. Worth-to-mention, the free-standing films did not show charge transport under dry conditions (*i.e.* very high electrical resistance). On a firsthand, this could be tentatively attributed to the arising of grain boundaries and/or fragmentation of the thin film into small domains (arising from the infiltration of Xanthan Gum into the conductive thin film) upon drying. Upon wetting the films, gum infiltrated gets solubilized cohering and healing the conductive thin film for charge carrier conduction.

Such effects of the hydration on the conductivity are inherent to melanin-inspired materials as presence of water in eumelanin materials promote the generation of ionic and radical species within the material (see Fig. 3a). On a first hand, an equilibrium between fully reduced catechol group (QH_2) and fully oxidized quinone (Q) groups found in eumelanin structures can occurs upon hydration giving rise to different protonated states and permitting thus proton conduction [35,36]. Furthermore, as humidity also reduces catechol moieties to semi-quinones (SQ) and several semi-quinone anions (SQ^-) inducing the formation of free-radicals which further contribute to the electronic charge carrier transport [20]. Other effects as stacking of aromatic cores (mediated by van der Waals, π-π stacking and hydrogen bonds) can also contribute to electron charge carrier conduction via electron hopping from aromatic to aromatic core [20]. Accordingly, natural eumelanin

typically exhibit semiconducting conductivity values of 10^{-2}-10^{-3} S cm^{-1} under dry conditions even over long millimetric distances [21,22]; and these values in natural eumelanin can be enhanced up to three orders of magnitude depending on the hydration conditions. Noteworthy, hydration increases eumelanin conductivity exponentially with small water increases [33]. Worth-to-mention, our MN-films show all high conductivities (without the need of dopants), good adhesion and biocompatibility which is hardly find in other melanin as shown in the comparison in Table S1 in the Supporting Information.

Remarkably, upon wetting our free-standing films with Phosphate Buffer Solution (PBS) in an attempt to mimic physiological sweat-like conditions [37], the measured sheet resistances proved to be much less dependent on the applied frequency presenting a constant plateau value around 6.6 ± 0.2 kΩ at low frequencies (Fig. 3c blue curve). These lower values may arise from the large concentration of ions and their strong contribution to the charge transport. Also, the presence of phosphate ions in the sweat-like conditions further contribute to the formation of different protonated state in the MN-film and hence increasing the previously commented proton conduction. Electrical DC measurements performed on the thin film under sweat-like conditions agree with this statement since larger sheet resistances of R_{sheet} = 55 ± 5 kΩ are obtained indicating a large ionic contribution as anticipated also in the AC measurements.

Finally, the electrical performance of the films was studied on a real pork skin as proof-of-concept. Untreated porcine skins were obtained from pig's flank within the 24 h post-mortem to ensure the highest resemblance to a living patient's skin. After several washes in MilliQ water, the dry MN-films were deposited on top of the wetted porcine skin and the excess of water gently removed by placing an absorbent tissue on top for a minute. Copper-tape contacts on polyimide substrates were mechanically deposited on top of the film and DC four-wire resistances were measured initially on flat samples under wetting conditions with pure water. Values of 228 ± 6 kΩ were obtained, similar to those previously found for the free-standing thin film. To assess the possible response of the e-skin device to body movement, the pork skin was afterwards fixed to a flexible substrate that can be bended either downwards or upwards with a bending radius of 17.5 cm (see Fig. 4a).

As the polyimide substrate with the copper contacts has a very large Young modulus, the device and contact geometry remains unchanged upon bending. Sheet resistance of the e-skin device under wet conditions decreased upon bending, with similar values for both upward and downward bending (175 ± 16 kΩ and 172 ± 18 kΩ, respectively). This effect has been recently studied and attributed to effects of compressing melanin-like films [38]. Upon contracting the MN-film as done when bending, desorption of the water molecules towards the surface of the film and compression of the conductive melanin domains occurs simultaneously. Therefore, a thinner layer of hydration is obtained enhancing the proton conduction and along with a more compact film

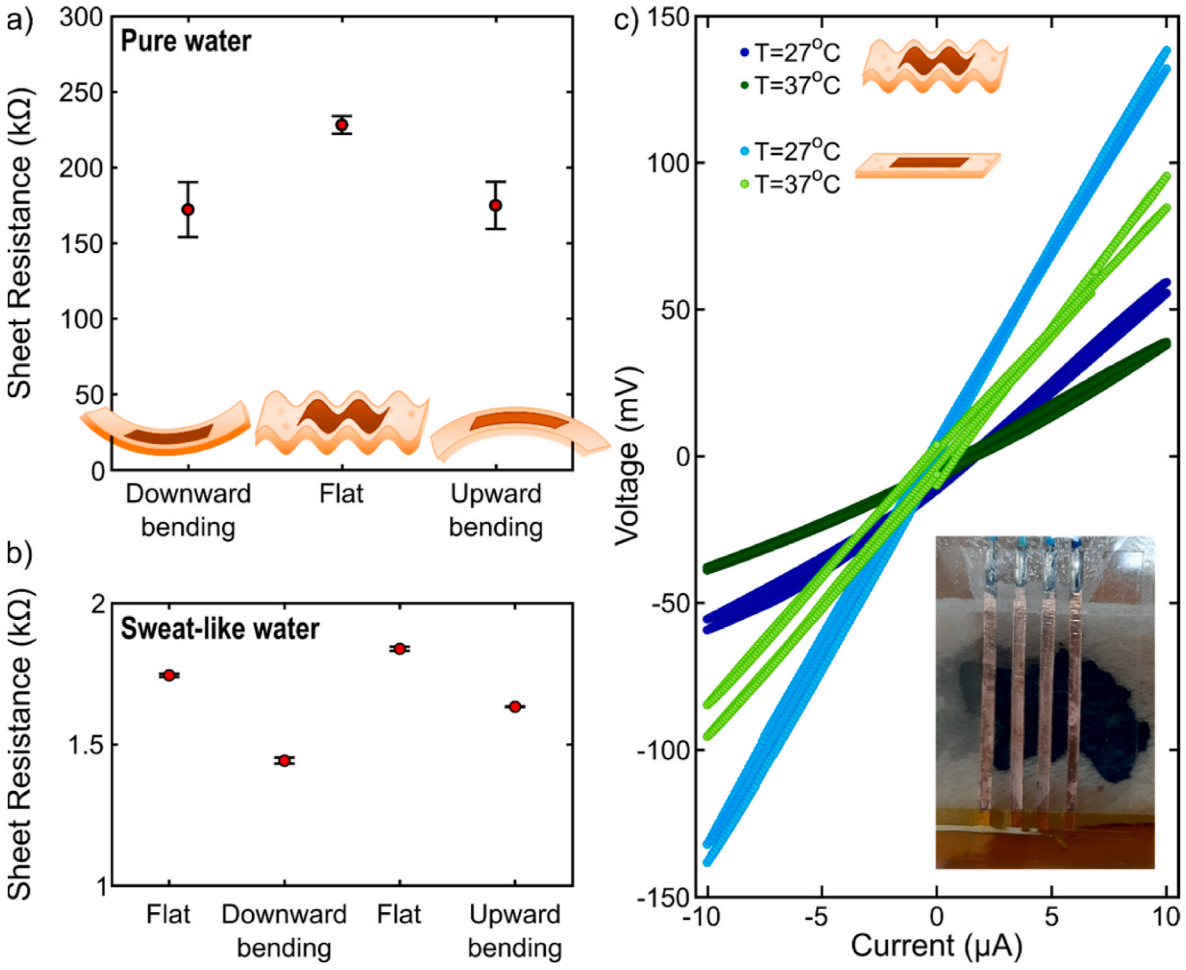

Fig. 4. (a) Measured four-wired sheet resistance values of melanin-inspired HHTP-based film wearable e-skin devices under pure water wetting conditions and under different bending conditions. Type and photographs of each bending are indicated underneath each measurement. (b) Measured four-wired sheet resistance values of e-skin devices under sweat-like wetting conditions and under different bending conditions indicated underneath each measurement. (c) Four-wire DC V–I curves of e-skin devices under sweat-like wetting conditions and under different linear stretching and temperature conditions. RT measurements can be found in blue and measurements at body-like temperatures are in green. Lighter colors correspond to stretching the skin at 15 %. (For interpretation of the references to color in this figure legend, the reader is referred to the Web version of this article.)

with better percolation between melanin domains which increases the electron conduction. Lower sheet resistances were obtained upon wetting the skin with PBS buffer emulating a physiological sweat-like conditions instead of water, as previously found for the free-standing thin MN-films. Four-wire DC measurements wetted with sweat-like buffer were also performed in the shown sequence: flat, bended downwards, flat again and bended upwards (Fig. 4b). The obtained values were 1.74 ± 0.01, 1.44 ± 0.01, 1.84 ± 0.01 and 1.63 ± 0.01 kΩ, respectively. Worth-to-mention, the measurements showcase a large reproducibility, with very low standard deviations, stating the stability of the film and electrode contacts within the working conditions. To evaluate the strain sensitivity of our films, we performed four-wire DC V–I measurements in relaxed and linear strained (estimated fixed strain at 15 %) flat positions of the pork skin under PBS wet conditions at room temperature (27 °C) (Fig. 4c light and dark blue curves).

The polyimide substrate with the copper contacts remained unstrained, thus electrode dimensions did not change. The pork skin with the film was stretched and fixed it mechanically and the contacts mechanically deposited afterwards; this procedure guarantees the same distance between electrodes even at large strain values of 15 %. Highly linear and reproducible V–I curves were obtained, indicating a clear sheet resistance dependence on the strain (*i.e.* increasing resistance at larger strain induced by the expansion of the film and the separation of melanin conductive domains). The estimated Gauge Factor (GF) was estimated to be GF~8.8 ($R^{0\%}_{sheet} = 13.8 \pm 0.8$ and $R^{15\,\%}_{sheet} = 32 \pm 1$ kΩ for normal and strained samples, respectively), indicating a large and good sensitivity for sensors to monitor body movement. Worth-to-mention, the obtained GF values are similar to those previously reported for related thin film-based e-skin devices [18] and even higher than hydrogel-based e-skin devices [25] and graphene-based tactile sensors [12]. These measurements were repeated at 37 °C emulating body temperature resulting in linear and reproducible V–I curves with sheet resistance values of $R^{0\%}_{sheet} = 9.1 \pm 0.2$ and $R^{15\,\%}_{sheet} = 21 \pm 2$ kΩ for relaxed and strained at 15 % e-skin devices respectively. This represents a conductivity increase in both cases though a similar value of the gauge factor with GF~8.7. Sheet resistance temperature dependence was also studied. A decrease for both relaxed and strained conditions upon increasing the temperature exhibited thermally activated behavior. The sensitivity to temperature was estimated calculating the temperature resistance coefficient of TRC = 3.4 %/K for both relaxed and strained conditions, independently of the stress applied to the e-skin device.

3. Conclusions

In summary, the results presented throughout this work show that largely conductive melanin-inspired free-standing thin films can be obtained by polymerization of HHTP catechol with a bisamine. The developed thin films exhibited a good electronic conductivity and performance under wet conditions, high biocompatibility with epithelial fibroblast cells and large adhesion and conformability towards porcine and human skin. Noteworthy, the films showcased dual charge carrier conduction giving rise to frequency variable conductivities of 15 ± 4 mS cm^{-1} and 0.5 ± 0.2 S cm^{-1} for low and high frequencies, respectively. Furthermore, the films could be implemented into porcine skin with an excellent performance, being sensitive to bending and stretching (regardless of the sweat content) and exhibiting a large gauge factor of GF = 8.8 independently of the applied temperature. Moreover, the film conductivity exhibited a remarkable temperature sensitivity (TCR = 3.4 % K^{-1}) under sweat-like conditions and independently of the applied strain, being potentially used not only for body motion (as for instance ECG or electromyogram) but also to temperature monitoring. Worth-to-mention, sensitivities to sweat, strain and temperature factors seemed to be independent, making selective sensing feasible while minimizing crosstalk. These results open the venue to melanin-inspired wearable e-skin devices in a real case scenarios as multifunctional sensing platform.

Credit author statement

Conceptualization, D.R.-M.; methodology N·C.-P. and S·S.-G.; formal analysis, N·C.-P. and S·S.-G; investigation, N·C.-P., R. P. and S·S.-G.; resources, D.R.-M.; data curation, N·C.P., R.P, D.R.M. and S·S.-G; writing—original draft preparation, N·C.-P.. and D.R.-M.; writing—review and editing, all the team; supervision, D.R.-M., S·S-G., N·C.-P., R.P.; project administration, D.R.-M., and S·S-G.; funding acquisition, D.R.-M. and S·S-G. All authors have read and agreed to the published version of the manuscript.

Declaration of competing interest

The authors declare the following financial interests/personal relationships which may be considered as potential competing interests. Daniel Ruiz Molina reports financial support was provided by Spain Ministry of Science and Innovation.

Data availability

Data will be made available on request.

Acknowledgements

The authors would like to acknowledge the funding support from grant PID2021-127983OB-C21 funded by MCIN/AEI/10.13039/501100011033 and by ERDF "A way of making Europe". The ICN2 is funded by the CERCA programme/Generalitat de Catalunya. The ICN2 is supported by the Severo Ochoa Centres of Excellence programme, Grant CEX2021-001214-S, funded by MCIN/AEI/10.13039.501100011033. Noemí Contreras Pereda's project that gave rise to these results received the support of a fellowship from "laCaixa" Foundation (ID 100010434). The fellowship code is LCF/BQ/ES17/11600012. R.P. acknowledges support from the Ramón y Cajal Fellowship (ref RyC2019-028474-I).

Appendix A. Supplementary data

Supplementary data to this article can be found online at https://doi.org/10.1016/j.mtchem.2023.101855.

References

[1] S.M.A. Mokhtar, E. Alvarez de Eulate, M. Yamada, T.W. Prow, D.R. Evans, Conducting polymers in wearable devices, Med Devices Sens 4 (2021), e10160, https://doi.org/10.1002/mds3.10160.
[2] W. Wu, L. Li, Z. Li, J. Sun, L. Wang, Extensible integrated system for real-time monitoring of cardiovascular physiological signals and limb health, Adv. Mater. (2023), 2304596, https://doi.org/10.1002/adma.202304596.
[3] M. He, W. Du, Y. Feng, S. Li, W. Wang, X. Zhang, A. Yu, L. Wan, J. Zhai, Flexible and stretchable triboelectric nanogenerator fabric for biomechanical energy harvesting and self-powered dual-mode human motion monitoring, Nano Energy 86 (2021), 106058, https://doi.org/10.1016/j.nanoen.2021.106058.
[4] C. Cui, Q. Fu, L. Meng, S. Hao, R. Dai, J. Yang, Recent progress in natural biopolymers conductive hydrogels for flexible wearable sensors and energy devices: materials, structures, and performance, ACS Appl. Bio Mater. 4 (2021) 85–121, https://doi.org/10.1021/acsabm.0c00807.
[5] B. Zhong, L. Wang, A stretchable cardiac ultrasound imager: a milestone in wearable bioimaging, Sci. Bull. 68 (2023) 868–870, https://doi.org/10.1016/j.scib.2023.04.002.
[6] L. Pan, P. Cai, L. Mei, Y. Cheng, Y. Zeng, M. Wang, T. Wang, Y. Jiang, B. Ji, D. Li, X. Chen, A compliant ionic adhesive electrode with ultralow bioelectronic impedance, Adv. Mater. 32 (2020), 2003723, https://doi.org/10.1002/adma.202003723.
[7] L. Chen, R. Li, S. Yuan, A. Chen, Y. Li, T. Zhang, L. Wei, Q. Zhang, Q. Li, Fiber-shaped artificial optoelectronic synapses for wearable visual-memory systems, Matter 6 (2023) 925–939, https://doi.org/10.1016/j.matt.2022.12.001.
[8] P. Guo, M. Jia, D. Guo, Z.L. Wang, J. Zhai, Retina-inspired in-sensor broadband image preprocessing for accurate recognition via the flexophototronic effect, Matter 6 (2023) 537–553, https://doi.org/10.1016/j.matt.2022.11.022.
[9] M. Wang, T. Wang, Y. Luo, K. He, L. Pan, Z. Li, Z. Cui, Z. Liu, J. Tu, X. Chen, Fusing stretchable sensing technology with machine learning for human–machine interfaces, Adv. Funct. Mater. 31 (2021), 2008807, https://doi.org/10.1002/adfm.202008807.

[10] R. Vo, H.H. Hsu, X. Jiang, Hydrogel facilitated bioelectronic integration, Biomater. Sci. 9 (2021) 23–37, https://doi.org/10.1039/d0bm01373k.
[11] S. Zhang, Z. Zhou, J. Zhong, Z. Shi, Y. Mao, T.H. Tao, Body-integrated, enzyme-triggered degradable, silk-based mechanical sensors for customized health/fitness monitoring and in situ treatment, Adv. Sci. 7 (2020), 1903802, https://doi.org/10.1002/advs.201903802.
[12] J. Kim, Y. Lee, M. Kang, L. Hu, S. Zhao, J. Ahn, 2D materials for skin-mountable electronic devices, Adv. Mater. 33 (2021), 2005858, https://doi.org/10.1002/adma.202005858.
[13] C. Wang, T. Yokota, T. Someya, Natural biopolymer-based biocompatible conductors for stretchable bioelectronics, Chem. Rev. 121 (2021) 2109–2146, https://doi.org/10.1021/acs.chemrev.0c00897.
[14] J.-N. Kim, J. Lee, T.W. Go, A. Rajabi-Abhari, M. Mahato, J.Y. Park, H. Lee, I.-K. Oh, Skin-attachable and biofriendly chitosan-diatom triboelectric nanogenerator, Nano Energy 75 (2020), 104904, https://doi.org/10.1016/j.nanoen.2020.104904.
[15] H. Tran, V.R. Feig, K. Liu, Y. Zheng, Z. Bao, Polymer chemistries underpinning materials for skin-inspired electronics, Macromolecules 52 (2019) 3965–3974, https://doi.org/10.1021/acs.macromol.9b00410.
[16] Z. Li, Y. Cui, J. Zhong, Recent advances in nanogenerators-based flexible electronics for electromechanical biomonitoring, Biosens. Bioelectron. 186 (2021), 113290, https://doi.org/10.1016/j.bios.2021.113290.
[17] Z. Li, M. Zhu, J. Shen, Q. Qiu, J. Yu, B. Ding, All-fiber structured electronic skin with high elasticity and breathability, Adv. Funct. Mater. 30 (2020), 1908411, https://doi.org/10.1002/adfm.201908411.
[18] P. Xiao, Y. Liang, J. He, L. Zhang, S. Wang, J. Gu, J. Zhang, Y. Huang, S.W. Kuo, T. Chen, Hydrophilic/hydrophobic interphase-mediated bubble-like stretchable janus ultrathin films toward self-adaptive and pneumatic multifunctional electronics, ACS Nano 13 (2019) 4368–4378, https://doi.org/10.1021/acsnano.8b09600.
[19] Y.R. Ding, C.H. Xue, Q.Q. Fan, L.L. Zhao, Q.Q. Tian, X.J. Guo, J. Zhang, S.T. Jia, Q. F. An, Fabrication of superhydrophobic conductive film at air/water interface for flexible and wearable sensors, Chem. Eng. J. 404 (2021), 126489, https://doi.org/10.1016/j.cej.2020.126489.
[20] A.B. Mostert, B.J. Powell, F.L. Pratt, G.R. Hanson, T. Sarna, I.R. Gentle, P. Meredith, Role of semiconductivity and ion transport in the electrical conduction of melanin, Proc. Natl. Acad. Sci. U. S. A. 109 (2012) 8943–8947, https://doi.org/10.1073/pnas.1119948109.
[21] M. d'Ischia, A. Napolitano, A. Pezzella, P. Meredith, M. Buehler, Melanin biopolymers: tailoring chemical complexity for materials design, Angew. Chem. Int. Ed. 59 (2020) 11196–11205, https://doi.org/10.1002/anie.201914276.
[22] M. Reali, A. Gouda, J. Bellemare, D. Ménard, J.-M. Nunzi, F. Soavi, C. Santato, Electronic transport in the biopigment sepia melanin, ACS Appl. Bio Mater. 3 (2020) 5244–5252, https://doi.org/10.1021/acsabm.0c00373.
[23] J. Ju, S. Jin, S. Kim, J.H. Choi, H.A. Lee, D. Son, H. Lee, M. Shin, Addressing the shortcomings of polyphenol-derived adhesives: achievement of long shelf life for effective hemostasis, ACS Appl. Mater. Interfaces 14 (2022) 25115–25125, https://doi.org/10.1021/acsami.2c03930.
[24] M.P. Sousa, A.I. Neto, T.R. Correia, S.P. Miguel, M. Matsusaki, I.J. Correia, J. F. Mano, Bioinspired multilayer membranes as potential adhesive patches for skin wound healing, Biomater. Sci. 6 (2018) 1962–1975, https://doi.org/10.1039/C8BM00319J.
[25] S. Hao, C. Shao, L. Meng, C. Cui, F. Xu, J. Yang, Tannic acid-silver dual catalysis induced rapid polymerization of conductive hydrogel sensors with excellent stretchability, self-adhesion, and strain-sensitivity properties, ACS Appl. Mater. Interfaces 12 (2020) 56509–56521, https://doi.org/10.1021/acsami.0c18250.
[26] Z. Xu, L. Chen, L. Lu, R. Du, W. Ma, Y. Cai, X. An, H. Wu, Q. Luo, Q. Xu, Q. Zhang, X. Jia, A highly-adhesive and self-healing elastomer for bio-interfacial electrode, Adv. Funct. Mater. 31 (2021), 2006432, https://doi.org/10.1002/adfm.202006432.
[27] J. Szewczyk, D. Aguilar-Ferrer, E. Coy, Polydopamine films: electrochemical growth and sensing applications, Eur. Polym. J. 174 (2022), 111346, https://doi.org/10.1016/j.eurpolymj.2022.111346.
[28] S. Ji, C. Wan, T. Wang, Q. Li, G. Chen, J. Wang, Z. Liu, H. Yang, X. Liu, X. Chen, Water-resistant conformal hybrid electrodes for aquatic endurable electrocardiographic monitoring, Adv. Mater. 32 (2020), 2001496, https://doi.org/10.1002/adma.202001496.
[29] X. Du, Z. Niu, R. Li, H. Yang, W. Hu, Highly adhesive, washable and stretchable on-skin electrodes based on polydopamine and silk fibroin for ambulatory electrocardiography sensing, J Mater Chem C Mater 8 (2020) 12257–12264, https://doi.org/10.1039/d0tc01940b.
[30] N. Contreras-Pereda, S. Pané, J. Puigmartí-Luis, D. Ruiz-Molina, Conductive properties of triphenylene MOFs and COFs, Coord. Chem. Rev. 460 (2022), 214459, https://doi.org/10.1016/j.ccr.2022.214459.
[31] S. Suárez-García, J. Sedó, J. Saiz-Poseu, D. Ruiz-Molina, Copolymerization of a catechol and a diamine as a versatile polydopamine-like platform for surface functionalization: the case of a hydrophobic coating, Biomimetics 2 (2017) 22, https://doi.org/10.3390/biomimetics2040022.
[32] S. Hong, C.F. Schaber, K. Dening, E. Appel, S.N. Gorb, H. Lee, Air/water interfacial formation of freestanding, stimuli-responsive, self-healing catecholamine janus-faced microfilms, Adv. Mater. 26 (2014) 7581–7587, https://doi.org/10.1002/adma.201403259.
[33] K.A. Motovilov, V. Grinenko, M. Savinov, Z.V. Gagkaeva, L.S. Kadyrov, A. A. Pronin, Z.V. Bedran, E.S. Zhukova, A.B. Mostert, B.P. Gorshunov, Redox chemistry in the pigment eumelanin as a function of temperature using broadband dielectric spectroscopy, RSC Adv. 9 (2019) 3857–3867, https://doi.org/10.1039/C8RA09093A.
[34] N. Contreras-Pereda, D. Rodríguez-San-Miguel, C. Franco, S. Sevim, J.P. Vale, E. Solano, W. Fong, A. Del Giudice, L. Galantini, R. Pfattner, S. Pané, T.S. Mayor, D. Ruiz-Molina, J. Puigmartí-Luis, Synthesis of 2D porous crystalline materials in simulated microgravity, Adv. Mater. 33 (2021), 2101777, https://doi.org/10.1002/adma.202101777.
[35] J.V. Paulin, S. Bayram, C.F.O. Graeff, C.C.B. Bufon, Exploring the charge transport of a natural eumelanin for sustainable technologies, ACS Appl. Bio Mater. 6 (2023) 3633–3637, https://doi.org/10.1021/acsabm.3c00469.
[36] J.V. Paulin, A.P. Coleone, A. Batagin-Neto, G. Burwell, P. Meredith, C.F.O. Graeff, A.B. Mostert, Melanin thin-films: a perspective on optical and electrical properties, J Mater Chem C Mater 9 (2021) 8345–8358, https://doi.org/10.1039/D1TC01440D.
[37] A.M. Foudeh, R. Pfattner, S. Lu, N.S. Kubzdela, T.Z. Gao, T. Lei, Z. Bao, Effects of water and different solutes on carbon-nanotube low-voltage field-effect transistors, Small 16 (2020), 2002875, https://doi.org/10.1002/smll.202002875.
[38] T. Vasileiadis, T. Marchesi D'Alvise, C.-M. Saak, M. Pochylski, S. Harvey, C. V. Synatschke, J. Gapinski, G. Fytas, E.H.G. Backus, T. Weil, B. Graczykowski, Fast light-driven motion of polydopamine nanomembranes, Nano Lett. 22 (2022) 578–585, https://doi.org/10.1021/acs.nanolett.1c03165.